COOKING POT HANDLE FRAGMENT V.008.2/2948.1. - LEADED BRONZE - ROMAN TIMES - SWITZERLAND

Artefact name Cooking pot handle fragment V.008.2/2948.1.

Authors Christian. Degrigny (HE-Arc CR, Neuchâtel, Neuchâtel, Switzerland) & Lucile. Ruynat (HE-Arc CR, None) & Valentin. Boissonnas (HE-Arc CR, Neuchâtel, Neuchâtel, Switzerland)

Url /artefacts/312/

The object

Fig. 1: Bronze cooking pot handle before and after treatment, front (a and c) and back (b and d),

Credit HE-Arc CR, L.Ruynat.

Description and visual observation

Description of the artefact

The object is the tip of a cooking pot handle representative of the Augustan age (100 AD), recognisable by the axial symmetry and the two orifices surrounded by prominent edging and flared shape. The upper part is composed of an openwork flower with three petals, comparable to the representation of the fleur-de-lis. A curved pattern frieze can be seen in the centre of the object. No decoration was found on the back. Before treatment, the object was covered with organic remains, most of which were mineralised (Figs. 1a and b)

Dimensions : L = 73 mm ; W = 48 ; T = 9 mm ; WT = 80.8 g.

Type of artefact Household implement

Origin Romans legionnaires' camp of Vindonissa (present-day town of Windisch), Aargau canton, CH., Windisch, Aargau, Switzerland

Recovering date 2008

Chronology category Roman Times

chronology tpq 1 A.D.

chronology taq 100 A.D.

Chronology comment 1st century AD

Burial conditions / environment	Soil
Artefact location	Archaeological Service of the Aargau canton, Brugg, Aargau
Owner	Archaeological Service of the Aargau canton, Brugg, Aargau
Inv. number	V.008.2/2948.1. (Inv. Number at HE-Arc: 2001)
Recorded conservation data	2008: Probably a first sediment clearing by archaeologists during the excavation. 2016-17: Lucile Ruynat, mechanical removal of the corrosion products over the limitos with ultrasonic scalpel. Conservation of wooden remains at the top right of the front of the object. Protective layer (varnish) with acrylic resin Paraloid B72®.

Complementary information

The soil of Windish is on the border between calcareous soil (Jura) and molasses-type (Swiss plateau). Calcareous soils tend to be alkaline whereas the molassic soil is generally more neutral. The Swiss climate is temperate, with the four marked seasons. It can have strong frosts in winter.

Study area(s)

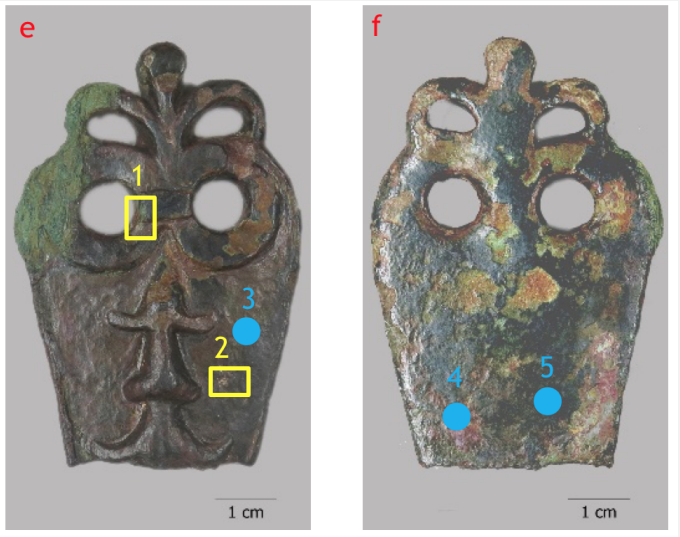

Credit HE-Arc CR, L.Ruynat.

Fig. 2: Cooking pot handle after treatment: front (e) and back (f). Location of sampling for SEM-EDS, Raman (yellow square 1), XRD analyses (yellow square 1 and 2), as well as the location of the XRF analyses (blue points 3, 4, 5),

Binocular observation and representation of the corrosion structure

The stratigraphy below gives an overview of the corrosion layers encountered on the object from visual macroscopic observation. The stratigraphy was created before treatment by observation under a binocular microscope and modified during the mechanical removal of corrosion products.

Fig. 3: Stratigraphic representation of the artefact in cross-section based on macroscopic global observation of the object. global observation of the object. S = structural void, CP = corrosion product, POM = pseudomorph of organic material, M = metal,

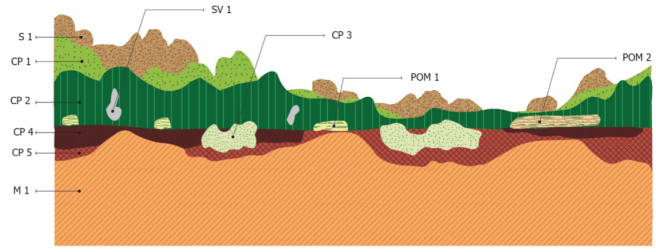

S1	Sediments with sand forming isolated and highly porous ochre-colored clusters
CP1	Scattered clusters of highly porous medium green corrosion product
CP2	Continuous layer of compact dark green corrosion product
SV1	Structural voids within CP2
POM1	Pseudomorphs of organic remains
POM2	Pseudomorphs of wood remains
CP3	Scattered clusters of highly porous light green corrosion product
CP4	Discontinuous layer of compact dark-red corrosion products
CP5	Discontinuous layer of compact red corrosion product
M1	Continuous and compact metal

Credit HE-Arc CR, L.Ruynat.

MiCorr stratigraphy(ies) – Bi

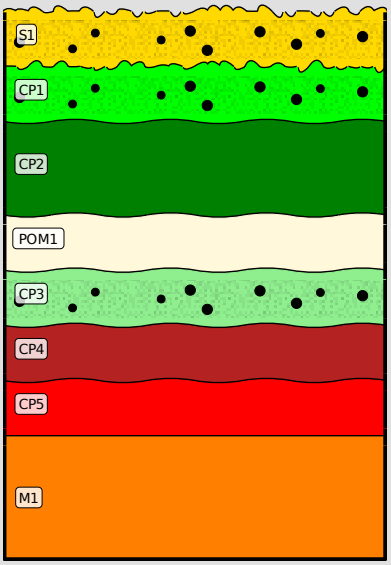

Fig. 4: Stratigraphic representation of the object in cross-section using the MiCorr application (to be compared to Fig. 3). The stratum is missing because it is integrated in CP2 and it was not possible to represent it in MiCorr while POM1 and POM2 are merged as POM1, Credit HE-Arc CR, L.Ruynat.

Sample(s)

Description of sample	No sample from the metal was removed. Only a few invasive samples were taken for analysis of corrosion products, as indicated on figure 2 (yellow square 1 and 2).
Alloy	Leaded Bronze
Technology	As-cast
Lab number of sample	
Sample location	None

Responsible institution	Archaeological Service of the Aargau canton, Brugg, Aargau
Date and aim of sampling	2017, chemical analyses

Analyses and results

XRF on the object with portable X-ray fluorescence spectrometer (NITON XL3t 950 Air GOLDD+ analyser, Thermo Fischer®).

XRD of powder samples using Stoe Mark II-Imaging Plate Diffractometer System (Stoe & Cie, 2015) equipped with a graphite-monochromator. Mo-Kα radiation (γ = 0.71073Å, beam diameter 0.5 mm, exposure time: 10 min).

SEM/EDS on the object.

Raman on powder samples of corrosion products.

SEM on sample of organic remains, as well as X-ray picture not presented in this report.

Non invasive analysis

Metal

The mechanical removal of corrosion products stopped at the limitos, so the metal was not directly observed. XRF analysis carried out after the cleaning process (Fig. 2, blue dot 3) showed that the metal is a leaded bronze (Table 1). Theoretically the metal is as-cast and should present a dendritic structure.

Elements mass %	Cu	Sn	Pb	Sb	Si	P	Ti	Fe
M1	61.1	21.1	14.2	0.9	0.9	0.4	0.2	0.1

Table 1: Chemical composition of the metal. Method of analysis: XRF, mode General metals, 60s (filters M20/Lo20/Li20). Located at point 3 Figure 2, credit MiCorr_HE-Arc CR, C.Degrigny.

Microstructure	Dendritic structure
First metal element	Cu
Other metal elements	Sn, Pb

Corrosion layers

Above the well-preserved metal core, CP4 is discontinuously interlocked in CP5. The XRD analysis done on a sample (Fig. 2, yellow square 2) of both corrosion products, shows that they are mainly constituted of cuprite (Cu2O), (Fig. 5). The colour difference can be explained by a tin enrichment in the darker CP4, as measured by XRF. XRF analysis of CP4 (Fig. 2, blue dot 5) and CP5 (Fig. 2, blue dot 4) is given in Table 2. The EDS analysis of the light green CP3 (yellow square 1 Fig. 2) layer did not reveal the presence of chlorides (Fig. 6). Complementary XRD analysis validated the absence of nantokite. Indeed the XRD and Raman indexing was not successful probably because the compound has a large

amorphous part. The other layers were not analysed, we expect CP1 and CP2 are malachite (carbonate hydroxyde) because of the green colour and absence of chlorides. Organic remains were mineralised and preserved by the corrosion process.

Elements mass %	Cu	Sn	Pb	Sb	As	Ag	Fe	P	Cl	S	BAL
Dark-red layer (CP4)	24.9	18.2	11.2	0.7	0.1	0.09	0.1	0.3	0.4	7.2	36.1
Red area layer (CP5)	33.5	14.5	16	0.5	0.8	0.1	0.05	1.3	0.6	1.5	30.5

Table 2: Chemical compositions of the dark-red and the red layers. Method of analysis: XRF, mode mining Cu/Zn, 180s (filters M30/Lo30/H60/Li60). BAL corresponds to the elements not analysed: O and C, credit MiCorr_HE-Arc CR, C.Degrigny.

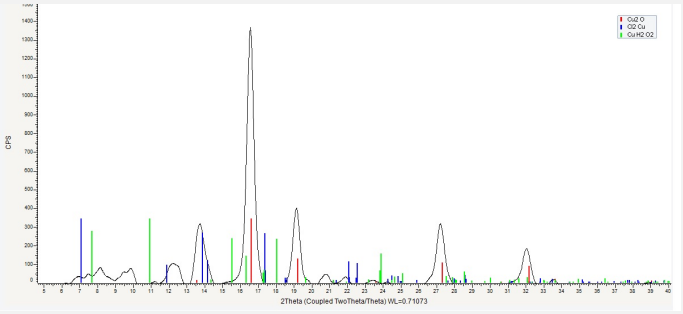

Credit Empa, A.Neels.

Fig.5: XRD spectrum of CP4 and CP5, Method of analysis: XRD, Center for X-ray Analytics, Empa,

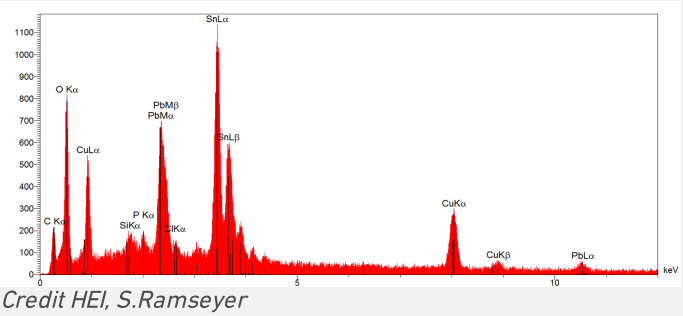

Credit HEI, S.Ramseyer

Fig. 6: EDS spectrum representative of the light green corrosion product (CP3). Method of analysis: SEM-EDS, Lab of Electronic Microscopy and Microanalysis, IMA (Néode), HEI Arc,

Corrosion form None

Corrosion type None

MiCorr stratigraphy(ies) – CS

Synthesis of the binocular / cross-section examination of the corrosion structure

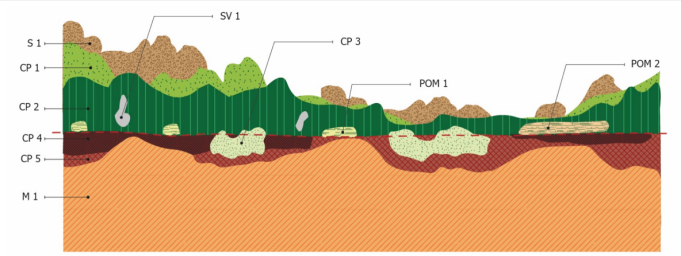

S1: Sediments	Soil and sand
CP1: Outer light green corrosion clusters	Malachite?
CP2: Outer dark green corrosion layer	Malachite?
SV1	Structural voids within CP2
POM1: Pseudomorphs of organic remains	Stems, grass within CP2
POM2: Pseudomorphs of organic remains	Wood within CP2
CP3: Outer/inner isolated light green corrosion product	No Nantokite, No Malachite
CP4: Inner black-dark red corrosion layer	Main phase: Cuprite Tin enrichment
CP5: Inner red corrosion layer	Main phase: Cuprite
M1: Orange Metal	Bronze with high lead content, probably with dendrites (as-cast)

Credit HE-Arc CR, L.Ruynat.

Fig. 7: Improved stratigraphic representation of the artefact from visual observations and analyses,

Conclusion

The object is a leaded bronze with a well-preserved metal core. Covering the metal are two strata (CP4 and CP5) composed of cuprite, the darker (CP4) appears enriched in tin. The superior interface of these layers represents the limitos. In areas the limitos, CP4 and CP5 have been replaced by a light green porous corrosion product (CP3). The following layers CP2 and CP1 are probably malachite.

The powdery green corrosion layer CP3 has frequently been observed on bronzes of Vindonissa where it can be located within cuprite or malachite layers. It is typically developed below the limitos and renders the latter extremely fragile. The nature of this corrosion product has not yet been determined. However, the absence of chlorine indicates that it is not a chlorinated corrosion product such as atacamite or paratacamite. The aggressive urban soil could be a reason for the transformation of these naturally grown and stable corrosion layers.

References

1. Käch. D. (2012) Jahresbericht 2011, Gesellschaft Pro Vindonissa, Brugg.

2. Käch, D. (2013) Jahresbericht 2012, Gesellschaft Pro Vindonissa, Brugg.

3. Holliger, C. (1984) "Bronzegefässe aus Vindonissa », In: Jahresbericht, Zürich, p.47-70.

4. Martin, M. (1994) Objets quotidiens de l'époque Romaine, Musée Romain d'Augst, Augst.

5. Feugere, M. (1994) « La vaisselle gallo-romaine en bronze de Vertault (Côte-d'Or) », In : Revue Archéologique de l'Est et du Centre-Est, p.137-166. [Consulté le 22.03.2016] https://halshs.archives-ouvertes.fr/halshs-00580295/document

6. Montandon, B. (1997) Le travail du bronze à l'époque Gallo-Romaine, In Chronozones, n°3, p.2-11.

7. Picon, M. et al. (1996) « Recherches techniques sur des bronzes de Gaule romaine ». In: Gallia, tome 24, n°1, p. 189-215.

8. Robbiola, L. et al. (1998) «Morphology and mechanisms of formation of natural patinas on archaeological Cu-Sn alloys», In Corrosion Science, N°40, p. 2083-2111

9. Robbiola, L. (1990) « Caractérisation de l'altération de bronzes archéologiques enfouis à partir d'un corpus d'objets de l'Age du bronze. Mécanismes de corrosion ». Thèse de Doctorat, Université Pierre et Marie Curie - Paris VI, Paris. In HAL archives ouvertes [En ligne]. HAL, 2010 [Consulté le 03.06.2017] https://tel.archives-ouvertes.fr/tel-00495356/document

10. Scott, D.A. (2002) Copper and bronze in Art, corrosion, colorants, conservation. Getty publications, Los Angeles.
11. Scott, D.A. (1987) « Metallography of Ancient Metallic Artifacts ». Institute of Archaeology, Summer Schools Press, London, pp. 3-17 and 128-132
12. Selwyn, L. (2004) Métaux et corrosion, un manuel pour le professionnel de la conservation. ICC-CCI, Ottawa.